Blends of Poly(meth)acrylates with 2-Oxo-(1,3)dioxolane Side Chains and Lithium Salts as Lithium Ion Conductors

Jochen Britz, Wolfgang H. Meyer, and Gerhard Wegner*

Max Planck Institute for Polymer Research, Ackermannweg 10, D-55128 Mainz, Germany

Received July 2, 2007; Revised Manuscript Received July 30, 2007

ABSTRACT: A novel approach is described to obtain polymers which show significant lithium ion conductivity when blended with lithium salts. Polymerization of acrylates and methacrylates with 2-oxo-1,3-dioxolane (cyclic carbonate) containing side chains gives polymers which contain the structural element of the prototypical solvent propylene carbonate (PC) firmly attached to the polymer host. (2-Oxo-1,3-dioxolane-4-yl)methyl methacrylate (DOMA) and the corresponding acrylate (DOA) were obtained by reaction of the (meth)acryloyl chloride with glycerol carbonate while (2-oxo-1,3-dioxolane-4-yl)butyl methacrylate (DOBMA) and the respective acrylate (DOBA) were obtained from the ω-hexenyl esters by first epoxidation followed by CO_2-insertion into the oxirane ring. Free radical polymerization in DMF gave the desired polymers. All homopolymers were thermally stable at least up to 200 °C; the glass transition temperature was found for PDOMA at 93 °C, for PDOA at 50 °C, for PDOBMA at 16 °C, and for PDOBA at 11 °C. Free radical copolymerization of DOMA with butyl methacrylate (BMA) ($r_1 = 1.24$, $r_2 = 0.80$) gave copolymers with T_g dependent on the BMA content. Blends of the homopolymers with lithium bis(trifluoro)methane sulfonimide (LiTFSI) gave appreciable lithium ion conductivities, particularly for blends of PDOA (3.7×10^{-6} S cm^{-1} at 40 °C) which could be substantially increased by further blending with small amounts of propylene carbonate. These blends of honey-like consistency showed conductivities of 1.8×10^{-3} S cm^{-1} (40 °C) for PDOA and 5.1×10^{-4} S cm^{-1} (40 °C) for PDOBMA each blended with LiTFSI and PC at equimolar amounts. The temperature dependence of lithium ion conductivity follows a WLF-type behavior in all cases; however, the reference temperatures do not bear any correspondence to the observed glass transition temperatures but are estimated from modified WLF-plots to be positioned in a temperature regime typical for local side chain relaxations in common polymers.

Introduction

The development of rechargeable lithium batteries has to be considered a milestone in the field of energy storage and supply for mobile and/or portable electrical and electronic devices. Lithium ions are solvated by an organic solvent in these batteries, and they diffuse freely between the two half-cells (anode and cathode compartments), which are physically isolated from each other by a separator membrane.[1,2] The latter prevents physical contact between the anode and cathode material, which would cause catastrophic discharging events. However, the membrane should not hamper transport of the solvated lithium ion between the two compartments during ordinary charging and discharging cycles of the device. Next to the choice of the appropriate materials for the electrodes, the selection of the optimal electrolyte is of outmost importance for a safe and efficient performance of the battery. Solutions of lithium salts in typical inert organic solvents have proven to be acceptable electrolytes for recyclable batteries. The requirement is that high ionic conductivity in the order of magnitude of 10^{-3} S cm^{-1} must be combined with high boiling point and low melting point to ensure safe performance over a wide temperature range.[3,4] Mixtures of ethylene carbonate (EC) and propylene carbonate (PC) have proven to fulfill reasonably well the requirements of safety and market concerns and are thus the solvents of choice for current commercial applications.[5,6] Lithium ions are solvated in these liquids with a tetrahedral solvent shell. In a mixture of EC and PC both compounds compete for placement in the first solvation shell around the lithium ion and the diameter of the effectively diffusing ion−solvent adduct has to be optimized choosing the best ratio of EC to PC in the system. However, free ions and solvent separated ion pairs are present in the actual electrolyte, and it is the concentration of free ions which eventually determines the macroscopic ionic conductivity. In practice, a compromise has to be achieved between optimizing the effective radius of the diffusing species and its concentration.[7−9] The dynamics of ion transport in such systems has been subject of extensive simulations, e.g., by Borodin and Smith.[10]

Lithium batteries which contain liquid organic electrolytes pose potential safety hazards in the case of abrupt leakage when mechanical forces are applied (e.g., in car accidents) or in the case of overheating in the course of sudden and uncontrolled discharge ("short circuits"). They require, therefore, preventive technical measures, such as relief valves and hermetic metal encasements. This results in an undesired decrease in the effective energy density of the lithium ion battery. The rigid encasement also interferes with the freedom to adapt the shape of the battery to the small size of modern portable electronic systems in which it has to fit. Moreover, some applications have been envisaged which ask for intrinsically flexible accumulators, which cannot be reconciled with a rigid housing.[11]

The problems encountered with highly fluid ("liquid") electrolytes could be avoided using polymers as lithium ion solvating matrix in batteries. Wright's discovery that alkali metal salt complexes of poly(ethylene oxide) (PEO) show substantial ionic conductivity was the starting point for extensive research to develop so-called solid polymer electrolytes (SPEs).[12] In fact, polymer electrolytes were proposed in 1978 for battery construction, because they combine advantages of solid-state electrochemistry with the ease of processing that is inherent to plastics.[13]

* Corresponding author. E-mail: wegner@mpip-mainz.mpg.de. Fax: ++49 (0)6131-379330.

10.1021/ma0714619 CCC: $37.00
Published on Web 09/20/2007

At this time one needs to differentiate three different approaches which are all found in current technology.[14,15]

(a) Dry SPEs: here, a polymer (mostly an ethylene oxide based material) serves as the host solvent for lithium salts. The polymer−salt complex functions only well at temperatures above its glass transition temperature that is in its visco-elastic state.

(b) Gel electrolytes: here, a polymer forms a porous matrix which contains the liquid electrolyte in its pores thereby immobilizing the liquid and preventing macroscopic flow (sudden leakage). The polymer itself does not contribute to the conductivity phenomena but is rather an inert frame by which compartmentation of the liquid is achieved.[16,17]

(c) Composite electrolytes: they contain a compaction of high surface area inorganic materials wetted at the surface with an ordinary organic electrolyte, a SPE or even a gel electrolyte. Ion mobility is generally much enhanced within the surface layers of ionic solids in contact with an electrolyte and the capillary effects acting between the particles serve to immobilize the liquid electrolyte against sudden leakage.

It is somewhat surprising to see that research on polymer solvents for lithium salts is almost completely focused on poly(alkylene oxides) with particular emphasis on poly(ethylene oxide) in its various architectures, e.g., block-, graft-, segmented-star-, etc. polymers and copolymers. While it was initially assumed that the crystalline domains formed by the PEO−salt complex are responsible for ion transport with the ions moving along PEO helices or channels formed by the PEO chains, it was soon established that it is solely the amorphous phase of the complexes which is responsible for conductivity.[18] The conductivity is thus related to the segmental motion of the polymer, and its temperature and frequency dependence scales with the glass transition phenomena.[14,19,20]

This restricts the principally achievable magnitude of lithium ion conductivity to values of the order $<10^{-4}$ S cm^{-1} at 30 °C.[21]

In the light that mixture of EC and PC have proven to be excellent solvents for lithium salts in today's large scale applications we were tempted to assume that polymers containing the structural element of EC and PC in their side chain would appear to be suitable polymeric solvents. The experience gained by research on PEO-based materials suggested that the structural elements which solvate the lithium ion should be dynamically detached as much as possible from the main chain of the polymer; in other words, a spacer between main chain and the side chain elements which are responsible for lithium ion solvation should assist in separating the main chain (polymer) dynamics from the motion of the side chain elements. It was, therefore, decided to synthesize a series of acrylates and methacrylates with 2-oxo-1,3-dioxolane (cyclic carbonate) containing side chains and study their potential as polymeric solvents of lithium salts in the context of the requirements for SPEs in lithium batteries. To the best of our knowledge, such polymers have not been prepared nor have their properties been tested.

Results and Discussion

Synthesis. The synthesis of two 2-oxo-1,3-dioxolane (cyclic carbonate) substituted methacrylate and acrylate monomers, respectively, is described in Scheme 1. The structures of the polymers obtained from these monomers are depicted in Table 1. Depending on the spacer length m, two different synthetic routes have been chosen. In the case of the spacer length $m = 1$, (2-oxo-1,3-dioxolane-4-yl)methyl methacrylate (DOMA) (**2**)[22−24] and (2-oxo-1,3-dioxolane-4-yl)methyl acrylate (DOA) (**3**)[22] are synthesized via esterification of (meth)acryloyl chloride and 4-hydroxymethyl-1,3-dioxolane-2-

Scheme 1. Synthesis of Various Cyclic Carbonate Substituted (Meth)acrylate Monomers

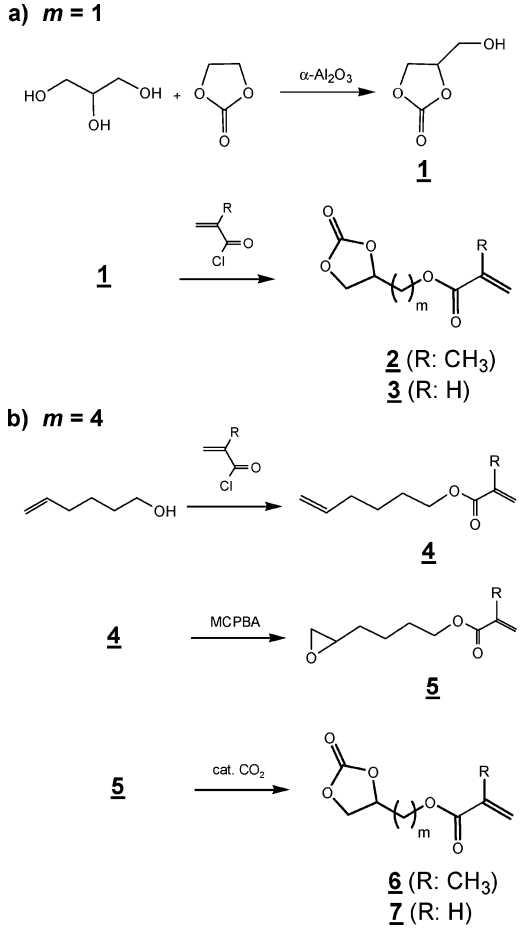

Table 1. Structures of the Relevant Homopolymers Synthesized and Investigated in This Work

	R = CH_3	R = H
m = 1	**8** Poly(2-oxo-[1,3]dioxolane-4-yl) methyl Methacrylate (PDOMA)	**9** Poly(2-oxo-[1,3]dioxolane-4-yl) methyl Acrylate (PDOA)
m = 4	**10** Poly(2-oxo-[1,3]dioxolane-4-yl) butyl Methacrylate (PDOBMA)	**11** Poly(2-oxo-[1,3]dioxolane-4-yl) butyl Acrylate (PDOBA)

Scheme 2. Synthesis of Homopolymers (Left) and Copolymers (Right)

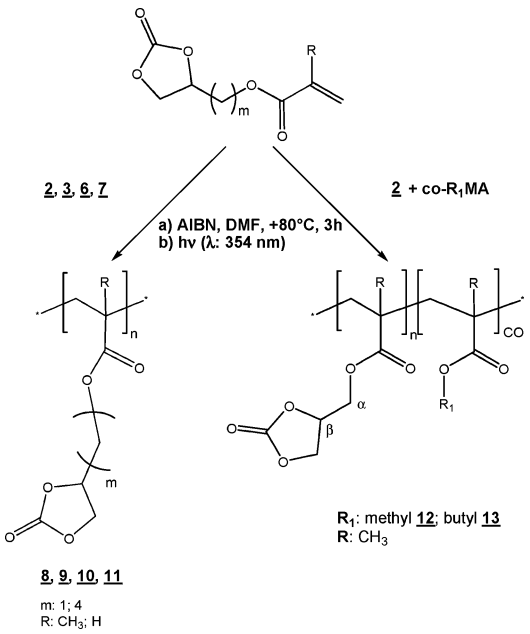

one (glycerol carbonate) (**1**), which is obtained by α-Al_2O_3 catalyzed transesterification of EC and glycerol.[25−27]

In contrast, monomers with the spacer length $m = 4$ are synthesized in a three step reaction: Esterification of (meth)-acryloyl chloride with ω-hexene-1-ol gives (hex-5-enyl)acrylate and − methacrylate (**4**), which are epoxidized by *m*-chloroperbenzoic acid (MCPBA) to yield (4-oxiranylbutyl)acrylate and -methacrylate (**5**). Finally **5** is converted into (2-oxo-1,3-dioxolane-4-yl)butyl methacrylate (DOBMA) (**6**) or respectively (2-oxo-1,3-dioxolane-4-yl)butyl acrylate (DOBA) (**7**) by transition metal catalyzed insertion of CO_2 into the epoxide ring.[24,28−30]

Scheme 2 shows the polymerization of the monomers **2**, **3**, **6**, and **7** to the homopolymers PDOMA (**8**), PDOA (**9**), PDOBMA (**10**), and PDOBA (**11**) as well as the copolymerization of **2** with methyl methacrylate (MMA) or butyl methacrylate (BMA) to P(DOMA-*co*-MMA) (**12**) and P(DOMA-*co*-BMA) (**13**). While the homopolymers were polymerized both free radically (FRP) and photochemically (PCP) via standard procedures under argon, the copolymers were exclusively polymerized free radically in order to stop the reaction more easily at low conversions of approximately 10%. This was necessary to acquire appropriate data to evaluate the copolymerization parameters.

In the synthesis of the monomers **6** and **7** with a spacer length of $m = 4$, it was essential that the esterification was performed prior to the epoxidation. Otherwise, the basic reaction conditions of the esterification lead to epoxide ring opening and formation of *trans*-1,2-dioles.

Moreover, a high regioselectivity for these particular epoxidations was observed: only the ω-double bonds and not the polymerizable α,β-double bonds of the acrylates and methacrylates are epoxidized at molar excess of MCPBA in diethyl ether.[31] This observation is a direct proof that the epoxidation mechanism via MCPBA is rather a concerted 1,3-dipolar suprafacially occurring [3 + 2]-cycloaddition as proposed by Kwart and Hoffman, and the addition mechanism suggested by Bartlett is not active under our conditions.[32,33]

Next, the CO_2-inserting reaction step was carried out using the system tributyltin iodide/tetrabutylammonium iodide.[24]

DOMA (**2**) was successfully anionically polymerized (AP) in dry THF using diphenyl lithium (DPHLi) as a starter. The same procedure did not work for acrylate monomers DOA (**3**) and DOBA (**7**) while for the butyl methacrylate DOBMA (**6**) a suitable solvent for the anionic polymerization could not be found.

Characterization of the Polymers. All obtained polymers are soluble in DMSO, DMF and PC. GPC experiments were carried out using the polymers dissolved in DMF with PMMA as calibration standard.

The GPC data (Table 2) demonstrate that the polymers have rather broad molecular weight distributions (PD) varying between 2.5−3.6 for the homo- and 1.9−2.8 for the copolymers, which is not uncommon for free radical polymerization.

Under the same homogeneous reaction conditions for FRP (1 mol % AIBN, 80 °C, 4 h), the highest molecular weights of PDOMA (**8**) have been obtained for DMF as a solvent. This can be explained invoking chain transfer to be an effective side reaction in the solvents THF, toluene or methanol leading to chain termination.[34] In consequence, DMF was chosen as most appropriate homogeneous solvent for all further experiments.

The data in Table 2 indicate that methacrylates generally give rise to polymers of much higher degrees of polymerization in comparison to acrylates. This agrees well with common experience.[34]

After fractional precipitation in cold diethyl-, di-*tert*-butyl ether, or methanol, filtration and drying at 80 °C in vacuo the polymers were characterized by ^{1}H and ^{13}C NMR-spectroscopy. The ^{1}NMR spectra of PDOA (**9**) and P(DOMA-*co*-BMA) (**13/11**) are displayed in Figure 1. One can clearly identify the β- and α-protons of the polymer backbone in the range of $\delta = 1.65-1.83$ ppm and $\delta = 2.28$ ppm in the case of **9**. The peak around $\delta = 4.27$ ppm represents an overlap of the two α-methylene protons of the acrylate and one proton of the methylene group of the 2-oxo-1,3-dioxolane cycle, whereas the second proton of this group is shifted to $\delta = 4.59$ ppm. For all polymers both the tertiary protons of the 2-oxo-1,3-dioxolane ring appear around $\delta = 5.05$ ppm and the signals for the four mentioned methylene protons are found at essentially the same position for all polymers. Additional peaks of **13/11** are located at $\delta = 3.89$, 1.58, 1.45, 0.91 ppm and are assigned to the α-, β-, γ-, and ω-protons of the alkyl chain of *B*MA. At $\delta = 0.91$ ppm these ω-protons of *B*MA overlap with signals of the methyl groups of the polymer backbone. The methyl group signal is split into different peaks indicating the tacticity of the chain. The syndiotactic sequences appear at around 0.78 ppm. Methacrylate β-protons of the polymer backbone significantly vary in the range of $\delta = 1.68-1.92$ ppm.

Thermal Properties. All homopolymers were stable at least up to 204 ± 8 °C when investigated by TGA under N_2 at a heating rate of 10 K min^{-1} (Figure 2). PDOA (**9**), PDOBMA (**10**), and PDOBA (**11**) appear to be more stable than PDOMA (**8**) namely up to 234 °C for the most thermally stable homopolymer **11** (see also Table 2). Variation in the onset temperatures of decomposition (T_d) for differently synthesized PDOMA (**8**) are explained by encapsulated traces of solvent in the polymer, which remain even after drying at 100 °C in vacuo for 1 week.

The glass transition temperatures were determined by DSC at a heating rate of 10 K min^{-1}. The data of all homopolymers are shown in Figure 3. T_g is found at + 11 °C in PDOBA (**11**) and at + 92 °C in PDOMA (**8/4**). A general trend can be stated as follows:

The polymers with the flexible butyl spacer have the lowest T_g and the samples with the short, more rigid tether the highest T_g. Furthermore, poly(acrylates) exhibit lower T_g than compa-

Table 2. Characteristic Data of the Synthesized Homo- and Copolymers

homopolymer	file no.	polymerization	solvent	M_n (10^3 g mol^{-1})	M_w (10^3 g mol^{-1})	PD[a]	T_d[b] (°C)	T_g[c] (°C)
PDOMA (**8**)	**8/1**	FRP[d]	THF	16	55	3.5	210	94
PDOMA	**8/2**	FRP	toluene	46	149	3.3	212	92
PDOMA	**8/3**	PCP[e]	methanol	33	113	3.4	200	93
PDOMA	**8/4**	FRP	DMF	77	191	2.5	198	92
PDOMA	**8/5**	AP[f]	THF	23	49	2.2	196	85
PDOA (**9**)	**9**	FRP	DMF	9	31	3.6	222	50
PDOBMA (**10**)	**10**	FRP	DMF	27	66	2.5	225	16
PDOBA (**11**)	**11**	FRP	DMF	3	11	3.6	234	11

P(DOMA-*co*-BMA) (**13**)

copolymer/molar ratio	file no.	polymerization	solvent	M_n (10^3 g mol^{-1})	M_w (10^3 g mol^{-1})	PD[a]	T_d[b] (°C)	T_g[c] (°C)
3:1	**13/31**	FRP	DMF	61	135	2.2	194	92
2:1	**13/21**	FRP	DMF	36	100	2.8	190	91
1:1	**13/11**	FRP	DMF	38	69	1.9	208	89
1:2	**13/12**	FRP	DMF	40	98	2.4	202	74
1:3	**13/13**	FRP	DMF	36	70	2.0	201	67
PBMA pure								20[34]

[a] Polydispersity index M_w/M_n by Gel Permeation Chromatography (GPC): Calibration standard: PMMA; RI detection. [b] Decomposition temperature by Thermogravimetric Analysis (TGA). [c] Glass transition temperature by Differential Scanning Calorimetry (DSC). [d] Free radical polymerization. [e] Photochemical polymerization. [f] Anionic polymerization: calculated for M_n = 20.000 g mol^{-1}.

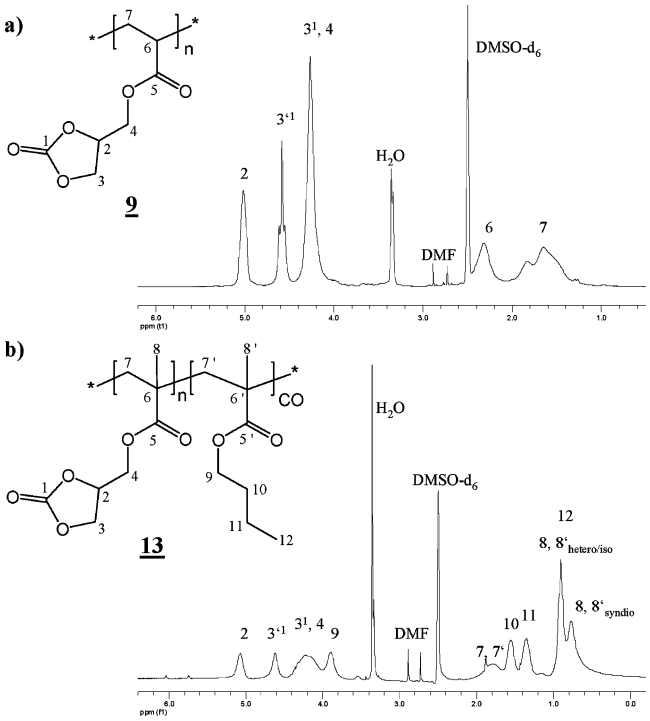

Figure 1. (a) ^{1}H NMR spectra of PDOA (**9**) and (b) P(DOMA-*co*-BMA) (**13/11**) (250 MHz, DMSO-d_6).

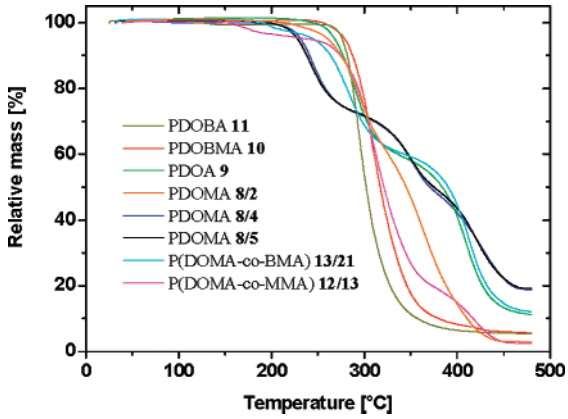

Figure 2. TGA traces of homopolymers and representative copolymers (under N_2 at a heating rate of 10 K min^{-1}). See Table 2 for explanation of file numbers, e.g., **8/2**.

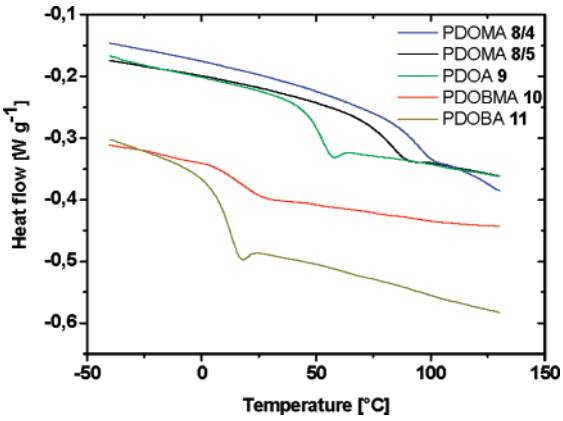

Figure 3. DSC traces of homopolymers (under N_2 at a heating rate of 10 K min^{-1}).

rable poly(methacrylates) due to a lower rigidity of the polymer backbone. This was expected and proves that the long tether gives rise to the highest local segment mobility at a given temperature.

Accordingly the copolymers showed increasing T_g with increasing amount of MMA in the copolymers. The opposite effect of a decreasing T_g with increasing molar ratio of BMA in the copolymers was observed in the case of P(DOMA-*co*-BMA) (**13**) (Table 2).

Copolymerization. Figure 4 displays the copolymerization diagram for the couple P(DOMA-*co*-BMA) (**13**). For the purpose of data collection, the copolymerization was stopped at low conversions of approximately 10% calculated by the half-life period of AIBN according to Cowie and traced by NMR spectroscopy.[35] Finally the molar ratio of DOMA in the copolymers was determined by evaluation of NMR integration ratios of the relevant signals and plotted vs the molar ratio of DOMA in the monomer mixture. All errors of this method are estimated at ±5%. The copolymerization diagram shown in Figure 4 demonstrates that the fit only slightly differs from the case of an ideal random copolymerization. Thus, the copolymers can be regarded as approximately random copolymers in the case of homogeneous monomer reaction mixtures.

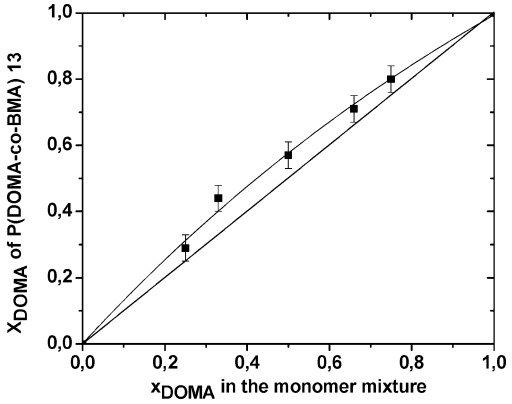

Figure 4. Copolymerization diagram of P(DOMA-*co*-BMA) (**13**) with a fit curve; error bars are indicated.

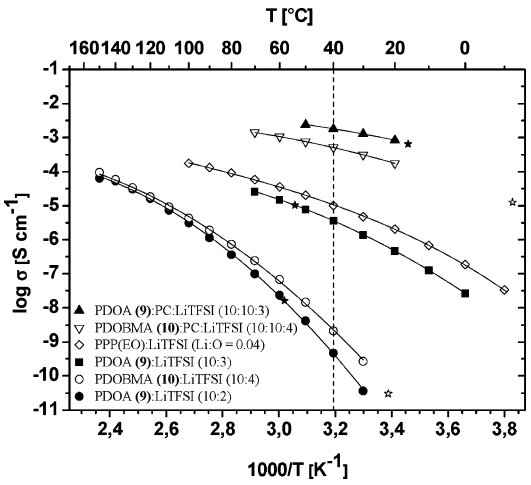

Figure 5. Temperature dependent conductivity of the homopolymer blends with LiTFSI and homopolymer blends additionally plasticized with PC in several molar ratios. The accordant T_gs are marked by stars. The data points (◇) are results of Lauter et al. relating to poly(*p*-phenylene)s with oligo(oxyethylene) side chains (PPP(EO)) blended with LiTFSI.[21]

According to the Lewis−Mayo equation, the copolymerization parameters of **13** are estimated as r_1(DOMA) = 1.24 ± 0.03 and r_2(BMA) = 0.80 ± 0.03.[36]

Lithium Ion Conductivity. Considerable conductivity is found for the homogeneously lithium salt blended homopolymers, reaching 1.2×10^{-4} S cm^{-1} at 150 °C in PDOBMA (**10**) and 2.6×10^{-5} S cm^{-1} at already 70 °C in PDOA (**9**) both of each blended with lithium bis(trifluoro)methane sulfonimide (LiTFSI) (LiN(SO_2CF_3)$_2$)[37,38] in molar ratios (polymer unit: LiTFSI) as indicated in Figure 5.

At a given temperature, the conductivity does not scale with spacer length; in other words, it is not observed that an increased spacer length between lithium ion solvating side groups and polymer backbone gives necessarily higher conductivity. This does not come unexpected since the fraction of free solvated ions will strongly depend on the dielectric constant of the medium which, in turn, will certainly decrease when a longer aliphatic spacer is present in the system. As pointed out in the Introduction, the conductivity arises as a subtle compromise between a number of different effects such that a naïve correlation with a structural feature as the spacer length does not work.[39−41] Thus, PDOBA (**11**) exhibits very poor lithium ion conductivity at the limits of detection.

However, the data of the other polymers which are collected in Figure 5 show the temperature dependence of conductivity in form of an Arrhenius plot, and they give evidence that appreciable conductivities can be reached which compare well with systems based on poly(ethylene oxide) as the solvating host. This is indicated in Figure 5 where literature data for a typical graft copolymer having oligo(oxyethylene) side chains blended with LiTFSI are shown for the sake of comparison.

Table 3. Glass Transition Temperatures, log σ (at 40 °C) and the Determined Fitting Parameters T_{ref}, A, and B of the Highest Obtained Lithium Ion Conductive Homopolymer (Plasticized) Blends (Eq 1)

sample	T_g (K)	log σ (40 °C) (S cm^{-1})	T_{ref} (K)	A (K$^{1/2}$)	B (10^3 K)
PDOA (**9**) pure	323				
PDOA (**9**):LiTFSI (10:2)	331	−9.33	227	20.9	0.81
PDOA (**9**):LiTFSI (10:3)	327	−5.43	167	22.9	0.82
PDOA (**9**):PC:LiTFSI (10:10:3)	289	−2.74	121	24.0	0.56
PDOBMA (**10**) pure	289				
PDOBMA (**10**):LiTFSI (10:4)	295	−8.67	216	21.9	0.85
PDOBMA (**10**):PC:LiTFSI (10:10:4)	261	−3.29	137	7762.5	1.85

A further very substantial enhancement of conductivity could be achieved when PDOA (**9**) doped with LiTFSI was plasticized with PC in a molar ratio of 1:1. As recorded in Table 3 the glass transition temperature decreased upon blending from 327 to 289 K while the conductivity at 40 °C increased by nearly 3 orders of magnitude. Similarly, when PDOBMA (**10**) doped with LiTFSI was plasticized with PC at a molar ratio of 1:1, T_g decreased by 34 K and the conductivity at 40 °C is increased by even more than 5 orders of magnitude to value of approximately 5×10^{-4} S cm^{-1}. The PC blended materials had the consistency of a very viscous, honeylike liquid.

It is worth noting that the effect of strong enhancement of conductivity by means of plasticizing with low molecular weight solvents for lithium salts had been observed by Lauter et al. for the case of the graft copolymers the data of which are quoted in Figure 5. In this case, blending of the oligo(oxyethylene) graft copolymers with oligoethers of the type of triglyme lead to an increase of conductivity of ca. 2.5 orders of magnitude at 40 °C.[21]

Returning to Figure 5, it is obvious that the temperature dependence of conductivity for the different systems does not follow a simple log(σ) ∼ T^{-1} behavior but a rather more complex correlation. Attempts to fit the data with a WLF algorithm using the observed glass transition temperature T_g as the reference temperature did not work as well. This is immediately obvious from the data contained in Figure 5, where the respective T_g for each system is indicated by an asterisk (see also Table 3 for the data). While the data obtained by Lauter et al. for the system composed of LiTFSI blended with a PEO graft copolymer could be well fitted with the WLF algorithm and T_g as the reference temperature as is indicated by the full line through the data points, a more complex algorithm was necessary to fit the data. We made use of a suggestion by Rössler and Sillescu to consider the temperature dependence of the viscosity of the medium in which the ion transport occurs by temperature-dependent preexponential factor to the WLF equation as follows:[42]

$$\log \sigma(T) = \frac{\log A}{\sqrt{T}} - \frac{B}{T - T_{ref}} \qquad (1)$$

In this equation A, B, and T_{ref} are phenomenological constants which need to be retrieved from the experimental data. More specifically, T_{ref} is not the glass transition temperature but relates

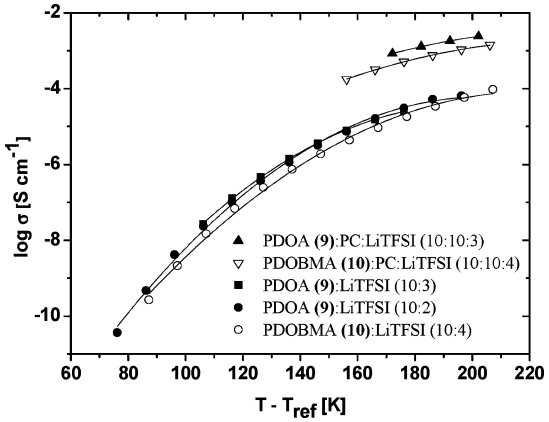

Figure 6. WLF plot of the lithium ion conductivity of homopolymer blends and blends plasticized by PC vs the reduced temperature $T-T_{ref}$. The parameters T_{ref}, A, and B needed to fit the data according to eq 1 are tabulated in Table 3.

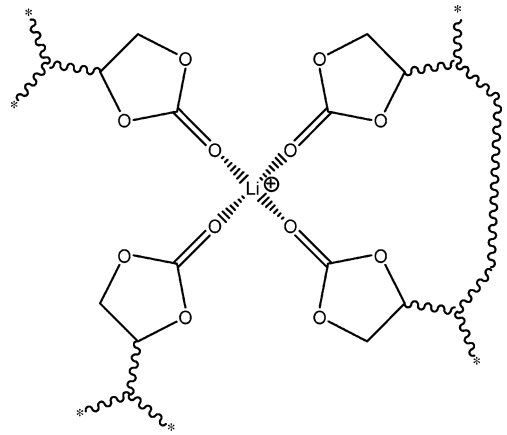

Figure 7. Suggested model of the lithium ion coordination in a cyclic carbonate substituted polymer matrix.

to the temperature at which the relaxation process which plays the major role in the ion transport through the host matrix will cease to be active ("freeze"). The full lines through the data points in Figure 5 represent the respective fits and the phenomenological constants A, B, and T_{ref} are tabulated in Table 3. T_{ref} was estimated from a preliminary fit of the data by a conventional WLF algorithm and the parameters A and B were then obtained by a best fit to eq 1. A plot of $\log(\sigma)$ vs $(T - T_{ref})$ is now able to produce a master curve type description (Figure 6). It is pleasing that the data of the homopolymers blends fall together within limits of error while the data of the systems plasticized with PC differ distinctively and appear to be shifted parallel to the ordinate by ca. 1 order of magnitude.

In the light of what is known on the structure of the solvation shell around the lithium ion and the dynamics of exchange of the solvate molecules, one is tempted to suggest a model in which the substituents at the backbone with their terminal cyclic carbonate groups coordinate at random with lithium ions (Figure 7). Exchange of solvate moieties can than be pictured as being linked to localized rotations of the terminal groups around a bond of the spacer. Such localized motions are typical for dipole relaxation modes in polymers and are independent of main chain segment relaxation modes. They typically start to be activated at temperatures much below the glass transition temperature.[43] Diffusion of lithium ions would be described as a random hopping process activated by fluctuations of the dipole density around the position of the ion. A direct prove of this surmise needs a combination of dielectric relaxation and NMR studies, which is presently under way in our laboratory.

Conclusions

While attempts to replace low molecular weight organic solvents for lithium salts in lithium based batteries were mostly concerned with poly(ethylene oxide) based polymers or polymer architectures containing oligo(ethylene oxide) segments we report here a novel approach to define a polymer solvent. In the light that mixtures of ethylene carbonate and propylene carbonate are accepted in practice as the most suitable solvent for common lithium salts to be used as the electrolyte in lithium batteries we demonstrate that a polymeric analogue of these solvents can be rationally and efficiently prepared. Free radical polymerization of acrylate and methacrylate esters which expose cyclic carbonate moieties in their ester side chain leads to high molecular weight polymers. These polymers have acceptable thermal stability at or above 200 °C and exhibit glass transition temperatures in the range typical for poly(acrylates) and poly(methacrylates) between 11 and 93 °C, the actual value depending on the structure of the main and side chains. All of these polymers are good solvents for lithium salts, e.g., lithium bis(trifluoro)methane sulfonimide, which is a common component of the supporting electrolyte in lithium batteries. Blends of the homopolymers with this salt gave very good ion conductivities as determined by impedance measurements. Addition of small amounts of propylene carbonate caused further and substantial increase in conductivity up to ca. 2×10^{-3} S cm^{-1} at 40 °C for poly(2-oxo-1,3-dioxolane-4-yl)methyl acrylate (PDOA).

The temperature dependence of ion conductivity follows a modified WLF-type behavior and is not of the Arrhenius-type. Somewhat surprising at first glance, the glass transition temperature of the polymer/salt blends does not serve as the reference temperature in a WLF-type treatment of the experimental data. Instead, the reference temperature is found to have values between 121 and 227 K that is more than 100 K below the actual T_g of the respective system. This points toward the ion mobility being controlled by side chain dipole relaxation modes which are quite typical for other aliphatic polymers having ester moieties in their side chains. In contrast, lithium ion mobility in poly(ethylene oxide)-type polymers is governed by main chain segment relaxation processes and, therefore, scales with T_g as the reference temperature in the temperature-dependent conductivity.

In agreement with findings on the state of complexation of the lithium ion dissolved in cyclic carbonates we are tempted to suggest that in the case of our polymers the lithium ion has a ligand sphere composed of four carbonate groups as schematically depicted in Figure 7. These ligands may be provided by different or the same polymer chain. In other words, at the present state of our investigations we cannot conclude on the ratio of inter- to intramolecular complexation of the lithium ion. However, transport of lithium ions in an electrochemical gradient must involve a kind of concerted hopping of the lithium ion activated by fluctuations of the dipole density around the position of the ion. Further studies which will also lead to optimization of the polymer structures and architectures vicinal conductivity need detailed NMR investigations on the type and rates of relaxation mechanisms. Such studies are currently under way in our laboratory.

Experimental Part

Materials. Chemicals were received from Acros, BASF, Fluka, Merck or Westfalen in p.a. quality and normally used without

further purification. DMF, THF, and toluene were dried and distilled under argon over sodium. Methanol, PC, methylene chloride, triethyl amine, and diethyl ether were dried with activated molecular sieves (4 Å).

For the radical and anionic polymerization all monomers were dried at 25 °C in vacuo of 8×10^{-5} mbar by an Alcatel CM Crystal diffusion pump setup. Thin Layer Chromatography was carried out with sheets from Machery-Nagel (silica gel 60 F254) and Merck (silica gel 60 silanized on glass) and usually exposed to iodine vapor or a potassium permanganate solution for visualization.

Measurements. The ^{1}H NMR and ^{13}C NMR spectra were recorded on Bruker AC-300 and Bruker Spectrospin 250 spectrometers at room temperature. Gel permeation chromatography (GPC) measurements were performed by a Waters WISP710B autosampler with coupled SDV columns from Polymer Standard Service (porosities: 10^2, 10^3, 3×10^3 Å) detected with UV (S-3702; SOMA) and RI (ERC 7512; ERMA) and calibrated with a PMMA standard. For FTIR-Measurements a Perkin-Elmer Paragon 1000 at a resolution of 4 cm^{-1} was used. Thermogravimetric Analysis (TGA) was measured under nitrogen at a heating rate of 10 K min^{-1} using a TGA/SDTA-851 (Mettler-Toledo). Differential scanning calorimetry (DSC) was carried out on a Mettler-Toledo DSC-30 under nitrogen at a heating rate of 10 K min^{-1}. Impedance spectroscopy (IS) was recorded as a function of temperature using a Solartron SI 1260 impedance / gain phase analyzer with a high-resolution dielectric converter (Alpha high-resolution dielectric analyzer; Novocontrol) in the range from $10^{-2}-10^7$ Hz. The measurements were performed using brass electrodes with a temperature controlled cryostat under nitrogen (Novocontrol). Dc-conductivities were usually obtained from Cole−Cole plots (Nyquist plot) at that point where the imaginary part of the conductivity ϵ'' was nil and in the case of the plasticized samples from the low-frequency plateau values of the real part of the ac-conductivities (Bode plot).

Preparation of the Blends. Solid homopolymer blends were dissolved in a small amount of dry DMF. Then these concentrated solutions were dropped onto coin-like brass electrodes with a diameter ranging from 10 to 20 mm to form thin films of a thickness of about 1 mm after complete evaporation of the organic solvent at 100 °C in vacuo being rechecked by NMR spectroscopy. Finally the counter electrodes were placed upon the thin films. Highly viscous (plasticized) homopolymer blends were placed between brass electrodes which were kept at a fixed distance of about 0.1 mm by means of a Teflon spacer.

Synthesis of the Monomers. (2-Oxo-1,3-dioxolane-4-yl)methyl Acrylate (DOA) (3). The synthesis of DOA (**3**) followed a slightly modified procedure of Katz.[22] In a two step reaction acryloyl chloride is esterified with 4-hydroxymethyl-1,3-dioxolane-2-one (**1**):[25−27] A solution of the glycerol carbonate (**1**) (14.1 g, 119 mmol) in 190 mL of THF and dry triethyl amine (12.0 g, 119 mmol) was cooled to 0 °C. Under argon acryloyl chloride (11.1 g, 119 mmol) in 70 mL of THF was carefully added to the stirring solution maintaining the temperature below 5 °C. After additional 10 min of stirring, the solution was filtrated, washed with a semisaturated NaCl solution and water and twice extracted with 150 mL of diethyl ether (DE). Drying over $MgSO_4$, evaporation of the organic solvents and further purification via column chromatography lead to colorless, viscous liquid **3** (8,6 g, 50 mmol).

(2-Oxo-1,3-dioxolane-4-yl)methyl Acrylate (3). Yield: 42%, retardation factor R_f (**3**, DE) = 0.64.

^{1}H NMR ($CDCl_3$, 250 MHz): $\delta = 4.27$ (dd, 1H, C^4,$^2J_{4,4'} = 12.6$ Hz,$^3J_{4,2} = 3.0$ Hz), 4.39 (dd, 1H, $C^{4'}$,$^2J_{4',4} = 12.6$ Hz,$^3J_{4',2} = 3.2$ Hz), 4.26−4.58 (m, 2H, C^3,$^3J_{3,2} = 8.5$ Hz), 4.94 (m, 1H, C^2,$^3J_{2,3} = 8.5$ Hz,$^3J_{2,4} = 3.0$ Hz,$^3J_{2,4'} = 3.2$ Hz), 5.88 (d, 1H, C^{7t},$^2J_{7t,7c} = 1.3$ Hz,$^3J_{7t,6} = 10.4$ Hz), 6.09 (t, 1H, C^6,$^3J_{6,7t} = 10.4$ Hz,$^3J_{6,7c} = 17.1$ Hz), 6.40 (d, 1H, C^{7c},$^2J_{7c,7\ t} = 1.3$ Hz,$^3J_{7c,6} = 17.1$ Hz).

^{13}C NMR ($CDCl_3$, 250 MHz): $\delta = 63.0$ (3-C), 65.9 (4-C), 73.8 (2-C), 127.0 (6-C), 132.5 (7-C), 154.4 (1-C), 165.3 (5-C).

IR (NaCl): $\lambda^{-1} = 3109$ (w, ν(=C−H)), 2991 (m, ν(C^2−H)), 2970 (m, ν(C−H)), 1799 (s, ν(O−C(=O)−O)), 1731 (s, ν(C=O)), 1637 (m, ν(C=C)), 1482, 1451, 1394 (m, δ(CH_2)), 1167, 1091, 1049 (s, ν(C−O−C)), 991 (s, δ(=C−H)), 771 (m, δ(CH_2)) cm^{-1}.

(2-Oxo-1,3-dioxolane-4-yl)butyl Methacrylate (DOBMA) (6). DOBMA (**6**) was synthesized in a three-step reaction. In analogy to the above-mentioned procedure by Katz,[22] at first a standard esterification of methacryloyl chloride (16.5 g, 153 mmol) and 5-hexene-1-ol (10.0 g, 99 mmol) in freshly distilled triethyl amine (47.1 g, 465 mmol) yielded, after acidifying with concentrated hydrochloric acid and further treatment, the yellow, viscous liquid **4** (14.6 g, 86 mmol).

(Hex-5-enyl)methacrylate (4). Yield: 87%.

^{1}H NMR ($CDCl_3$, 250 MHz): $\delta = 1.45$ (m, 2H, C^7,$^3J_{7,6} = 7.0$ Hz,$^3J_{7,8} = 7.3$ Hz), 1.65 (m, 2H, C^6,$^3J_{6,5} = 6.3$ Hz,$^3J_{6,7} = 7.0$ Hz), 1.93 (s, 3H, C^4), 2.06 (m, 2H, C^8,$^3J_{8,7} = 7.3$ Hz,$^3J_{8,9} = 7.0$ Hz), 4.11 (t, 2H, C^5,$^3J_{5,6} = 6.3$ Hz), 4.93 (d, 1H, C^{10t},$^2J_{10t,10c} = 1.9$ Hz,$^3J_{10t,9} = 10.1$ Hz), 4.99 (d, 1H, C^{10c},$^2J_{10c,10t} = 1.9$ Hz,$^3J_{10c,9} = 17.1$ Hz), 5.52 (s, 1H, C^{1t}), 5.77 (m, 1H, C^9,$^3J_{9,8} = 7.0$ Hz,$^3J_{9,10c} = 17.1$ Hz,$^3J_{9,10t} = 10.1$ Hz), 6.06 (s, 1H, C^{1c}).

^{13}C NMR ($CDCl_3$, 250 MHz): $\delta = 17.5$ (4-C), 24.2 (7-C), 27.6 (6-C), 32.9 (8-C), 63.4 (5-C), 114.1 (10-C), 124.7 (1-C), 136.7 (2-C), 138.2 (9-C), 167.1 (3-C).

IR (NaCl): $\lambda^{-1} = 3105$ (w, ν(=C^{1}−H)), 3080 (m, ν(=$C^{9,10}$−H)), 2955 (m, ν(C−H, CH_3)), 2934 (m, ν(C−H, CH_2)), 1724 (s, ν(C=O)), 1640, 1638 (m, ν(C=C)), 1440, 1438, 1382 (m, δ(CH_2, CH_3)), 1164 (s, ν(C−O−C)), 990, 942, 911 (s, δ(=C−H)), 821 (m, δ(CH_2)) cm^{-1}.

In the second reaction step, **4** (12.4 g, 72 mmol) was added at 0 °C to a solution of MCPBA (19.7 g, 80 mmol) in 100 mL of DE maintained under vigorous stirring for 24 h. After complete epoxidation, the solution was twice washed with 10 wt % sodium hydroxide solution and water and dried over $MgSO_4$, and the organic solvent was evaporated off. A sufficient purification was achieved in vacuo by means of a cryo trap yielding a colorless, viscous liquid, **5** (9.2 g, 50 mmol).

(4-Oxiranylbutyl)methacrylate (5). Yield: 70%.

^{1}H NMR ($CDCl_3$, 250 MHz): $\delta = 1.54$ (m, 2H, C^4,$^3J_{4,3} = 6.6$ Hz,$^3J_{4,5} = 6.6$ Hz), 1.60 (m, 2H, C^3,$^3J_{3,4} = 6.6$ Hz), 1.68 (m, 2H, C^5,$^3J_{5,4} = 6.6$ Hz,$^3J_{5,6} = 6.3$ Hz), 1.89 (s, 3H, C^{10}), 2.45 (dd, 1H, C^1,$^2J_{1,1'} = 3.8$ Hz,$^3J_{1,2} = 1.6$ Hz), 2.73 (dd, 1H, $C^{1'}$,$^2J_{1',1} = 3.8$ Hz,$^3J_{1',2} = 1.6$ Hz), 2.89 (m, 1H, C^2,$^3J_{2,1;\ 2,1'} = 1.6$ Hz), 4.11 (t, 2H, C^6,$^3J_{6,5} = 6.3$ Hz), 5.51 (s, 1H, C^{9t},$^2J_{9t,9c} = 1.4$ Hz), 6.05 (s, 1H, C^{9c},$^2J_{9c,9t} = 1.4$ Hz).

^{13}C NMR ($CDCl_3$, 250 MHz): $\delta = 18.1$ (10-C), 20.9 (4-C), 27.9 (5-C), 33.2 (3-C), 47.5 (1-C), 50.4 (2-C), 64.9 (6-C), 125.3 (9-C), 136.0 (8-C), 167.2 (7-C).

IR (NaCl): $\lambda^{-1} = 3106$ (w, ν(=C−H)), 2956 (m, ν(C−H, CH_3)), 2932 (s, ν(C^2−H, CH_2)), 1726 (s, ν(C=O)), 1640 (m, ν(C=C)), 1469, 1439, 1408 (m, δ(CH_2,CH_3)), 1261, 1164 (s, ν(C−O−C)), 942 (s, δ(=C−H)), 836, 818 (m, δ(CH_2)) cm^{-1}.

Finally, **5** (9.2 g, 50 mmol) was homogeneously mixed with tributyltin iodide (0.8 g, 2 mmol), tetrabutylammonium iodide (0.7 g, 2 mmol), 10 mL of DE, and catalytic amounts of inhibiting hydroquinone. Under nitrogen and stirring CO_2 was continuously bubbled into the viscous solution for 14 h at 40 °C. After complete CO_2 addition the reaction mixture was extracted with 150 mL of DE, neutralized with semisaturated $NaHCO_3$ solution, washed with water, and dried over $MgSO_4$. Evaporation of DE and purification by means of column chromatography lead to the colorless, highly viscous liquid **6** (3.2 g, 14 mmol).[24]

(2-Oxo-1,3-dioxolane-4-yl)butyl Methacrylate (DOBMA) (6). Yield: 28%; R_f(**6**, DE) = 0.54.

^{1}H NMR ($CDCl_3$, 250 MHz): $\delta = 1.52$ (m, 2H, C^5,$^3J_{5,4} = 6.7$ Hz,$^3J_{5,6} = 7.9$ Hz), 1.65 (m, 2H, C^6,$^3J_{6,5} = 7.9$ Hz,$^3J_{6,7} = 6.3$ Hz), 1.74 (m, 2H, C^4,$^3J_{4,2} = 7.6$ Hz,$^3J_{4,5} = 6.7$ Hz), 1.90 (s, 3H, C^{11}), 4.07 (dd, 1H, C^7,$^2J_{7,7'} = 12.7$ Hz,$^3J_{7,6} = 6.3$ Hz), 4.12 (dd, 1H, $C^{7'}$,$^2J_{7',7} = 12.7$ Hz,$^3J_{7',6} = 6.3$ Hz), 4.03−4.50 (m, 2H, C^3,$^2J_{3,3'} = 8.2$ Hz,$^3J_{3,2} = 7.3$ Hz), 4.68 (m, 1H, C^2,$^3J_{2,3} = 7.3$ Hz,$^3J_{2,4} = 7.6$ Hz), 5.52 (s, 1H, C^{10t}), 6.04 (s, 1H, C^{10c}).

^{13}C NMR ($CDCl_3$, 250 MHz): $\delta = 18.2$ (11-C), 21.1 (5-C), 28.0 (6-C), 33.4 (4-C), 63.8 (7-C), 69.2 (3-C), 76.7 (2-C), 125.4 (10-C), 136.1 (9-C), 154.9 (1-C), 167.3 (8-C).

IR (NaCl): $\lambda^{-1} = 3100$ (w, ν(=C−H)), 2980 (m, ν(C^2-H), 2960 (m, ν(C−H, CH_3)), 1794 (s, ν(O−C(=O)-O)), 1723 (s, ν(C=O)), 1640 (m, ν(C=C)), 1483, 1454, 1390 (m, δ(CH_2,CH_3)), 1169, 1122, 1050 (s, ν(C−O−C)), 940 (s, δ(=C−H)), 776 (m, δ(CH_2)) cm^{-1}.

Synthesis of the Polymers. All radical polymerizations were carried out by the following general procedure.

The purified and well dried monomers (1 g) were dissolved in 5 g of dry DMF. Under argon and exclusion of moisture 1 mol % AIBN was added and the reaction mixture was maintained at 80 °C for 4 h. The polymers were obtained by precipitation in little cold methanol and characterized after filtration and drying at 100 °C in vacuo for at least 1 week.

Poly(2-oxo-1,3-dioxolane-4-yl)methyl Acrylate (PDOA) (9). Yield: 87%.

^{1}H NMR (DMSO-d_6, 250 MHz): δ = 1.65−1.82 (d^b, $(2H)_n$, C^7), 2.32 (s^b, $(1H)_n$, C^6), 4.27 (s^b, {$(1H)_n$, C^3}, {$(2H)_n$, C^4}), 4.59 (t^b, $(1H)_n$, $C^{3'}$), 5.02 (s^b, $(1H)_n$, C^2).

^{13}C NMR (DMSO-d_6, 250 MHz): δ = 38.9 (7-C), 41.2 (6-C), 64.2 (3-C), 66.4 (4-C), 74.6 (2-C), 155.1 (1-C), 173.9 (5-C).

IR (KBr): $\lambda^{-1} = 2991$ (m, ν(C^2-H)), 2970 (m, ν(C−H)), 1800 (s, ν(O−C(=O)-O)), 1731 (s, ν(C=O)), 1482, 1451, 1395 (m, δ-(CH_2)), 1167, 1090, 1050 (s, ν(C−O−C)), 772 (m, δ(CH_2)) cm^{-1}.

Poly(2-oxo-1,3-dioxolane-4-yl)butyl Methacrylate (PDOBMA) (10). Yield: 86%.

^{1}H NMR (DMSO-d_6, 250 MHz): δ = 0.77−0.95 (d^b, $(2H)_n$, C^{10}), 1.44−1.71 (m^b, 3 $(2H)_n$, C^5, C^6, C^4, $(3H)_n$, C^{11}), 4.04 (s^b, {-$(1H)_n$, C^7}, {$(1H)_n$, C^3}), 4.14 (s^b, $(1H)_n$, $C^{7'}$), 4.58 (s^b, $(1H)_n$, $C^{3'}$), 4.79 (s^b, $(1H)_n$, C^2).

^{13}C NMR (DMSO-d_6, 250 MHz): δ = 20.5 (11-C), 27.0 (5-C), 32.1 (6-C), 38.2 (4-C), 40.1 (10-C), 43.8 (9-C), 68.8 (7-C), 71.8 (3-C), 76.6 (2-C), 154.5 (1-C), 176.4 (8-C).

IR (KBr): $\lambda^{-1} = 2989$ (m, ν(C^2-H)), 2960 (m, ν(C−H, CH_3)), 1795 (s, ν(O−C(=O)-O)), 1724 (s, ν(C=O)), 1483, 1454, 1390 (m, δ(CH_2,CH_3)), 1240, 1121, 1050 (s, ν(C−O−C), 775 (m, δ-(CH_2)) cm^{-1}.

Acknowledgment. The authors gratefully acknowledge assistance in the synthetic work by A. Manhart and in retrieving the impedance spectra by C. Sieber. S. Seywald and E. Muth are acknowledged for assistance in obtaining polymer analytical data.

References and Notes

(1) Zhang, S. S. *J. Power Sources* **2007**, *164*, 351.
(2) Baril, D.; Michot, C.; Armand, M. B. *Solid State Ionics* **1997**, *94*, 35.
(3) Krieger, J. *Chem. Eng. News* **1992**, *16*, 17.
(4) *Battery Test Procedure Manual*; USABC: Southfield, MI, 1994.
(5) Tsutsumi, H.; et al. *Solid State Ionics* **2003**, *160*, 131.
(6) Li, X.; Goh, S. H.; Lai, Y. H.; Deng, S. M. *J. Appl. Polym. Sci.* **1999**, *73*, 2771.
(7) Li, T.; Balbuena, P. B. *J. Electrochem. Soc.* **1999**, *146*, 3613.
(8) Izutsu, K.; Nakamura, T.; Miyoshi, K.; Kurita, K. *Electrochim. Acta* **1996**, *41*, 2523.
(9) Wagner, M. R.; Albering, J. H.; Moeller, K.-C.; Besenhard, J. O.; Winter, M. *Electrochem. Commun.* **2005**, *7*, 947.
(10) Borodin, O.; Smith, G. D. *J. Phys. Chem. B* **2006**, *110*, 4971.
(11) *Fraunhofer ISIT, Annual Report*; Sollith Batteries GmbH: Itzehoe, Germany; and Bullith Batteries AG: München, Germany, 2004; p 69.
(12) Fenton, D. E.; Parker, J. M.; Wright, P. V. *Polymer* **1973**, *14*, 589.
(13) Armand, M.; Duclot, M. French Patent 7832976, 1978.
(14) Meyer, W. H. *Adv. Mater.* **1998**, *10*, 439.
(15) Dias, F. B.; Plomp, L.; Veldhuis, J. B. *J. Power Sources* **2000**, *88*, 169.
(16) Lee, S.-Y.; Meyer, W. H.; Wegner, G. *ChemPhysChem.* **2005**, *6*, 49.
(17) Lee, S.-Y.; Scharfenberger, G.; Meyer, W. H.; Wegner, G. *Adv. Mater.* **2005**, *17*, 626.
(18) Berthier, C.; Gorecki, W.; Minier, M.; Armand, M. B.; Chabagno, J. M.; Rigaud, P. *Solid State Ionics* **1983**, *11*, 91.
(19) Armand, M. B. *Solid State Ionics* **1994**, *69*, 309.
(20) Abraham, K. M. *Electrochim. Acta* **1993**, *38*, 1233.
(21) Lauter, U.; Meyer, W. H.; Wegner, G. *Macromolecules* **1997**, *30*, 2092.
(22) Katz, H. D. *Macromolecules* **1987**, *20*, 2026.
(23) Fang, J. C. (duPont de Nemours & Co.) U.S. 2,967,173; *Chem. Abstr.* **1961**, 7909.
(24) Baba, A.; Nozaki, T.; Matsuda, H. *Bull. Chem. Soc. Jpn.* **1987**, *60*, 1552.
(25) Sugita, A.; Sone, Y.; Kaeryama, M. Patent Jpn. Kokai Tokkyo Koho JP 06329663, 1994.
(26) Sugita, A.; Sone, Y.; Kaeryama, M. Patent Jpn. Kokai Tokkyo Koho JP 3540822, 2004.
(27) Mouloungui, Z.; Yoo, J. W.; Gachen, C. A.; Gaset, A.; Vermeersch, G. Eur. Pat. Appl. 1996, EP 739888.
(28) Kossev, K.; Koseva, N.; Troev, K. *J. Mol. Catal. A* **2003**, *194*, 29.
(29) Yu, B.; Jeong, E.; Kim, I.; Kim, M.; Oh, K.; Park, D. W. *Catal. Today* **2004**, *98*, 499.
(30) Shin, D.; Kim, J.; Woo, H.; Lim, D.; Park, D. W. *React. Kinet. Catal. Lett.* **2003**, *79* (*2*), 233.
(31) De Cock, C.; De Keyser, J.; Poupaert, J.; Dumont, P. *Bull. Soc. Chim. Belg.* **1987**, *96* (10), 783.
(32) Kwart, H.; Hoffman, D. M. *J. Org. Chem.* **1966**, *31*, 419.
(33) Bartlett, P. D. *Rec. Chem. Progr.* **1957**, *18*, 111.
(34) Ueda, A.; Nagai, S.; et al. In *Polymer Handbook*, 4th ed.; Brandrup, J., Immergut, E. H., Grulke, E. A., Eds.; Wiley-Interscience: Hoboken, NJ, 1999; Vol. 1/2, p II/97.
(35) Cowie, J. M. *Chemie und Physik der Polymere*; Vieweg: Braunschweig and Wiesbaden, Germany, 1997; p 59.
(36) Lewis, F. M.; Mayo, F. R.; Hulse, W. F. *J. Am. Chem. Soc.* **1945**, *67*, 1701.
(37) Roux, C.; Gorecki, W.; Sanchez, J. Y.; Jeannin, M.; Belorizky, E. *J. Phys.: Condens. Matter* **1996**, *8*, 7005.
(38) Labrèche, C.; Lévesque, I.; Prud'homme, J. *Macromolecules* **1996**, *29*, 7795.
(39) Bruce, P. G.; Vincent, C. A. *Faraday Discuss. Chem. Soc.* **1989**, *88*, 43.
(40) Cohen, M. H.; Turnbull, D. *J. Chem. Phys.* **1959**, *31*, 1164.
(41) Ratner, M. A. In *Polymer Electrolyte Reviews I*; MacCallum, J. R., Vincent, C. A., Eds.; Elsevier, 1987; p 173.
(42) Rössler, E.; Sillescu, H. In *Materials Science and Technology*; Cahn, R. W., Haasen, P., Kramer, E. J., Eds.; Wiley: New York, 2005; Vol. 8/9, Chapter 11, p 573.
(43) McCrum, N. G.; Read, B. E.; Williams, G. In *Anelastic and Dielectric Effects in Polymeric Solids*; Wiley: London, 1967; Chapter 8, p 238.

MA0714619